Ref. Ares(2026)9854238 - 20/10/2026

BE-LIGHT

Improving biomedical diagnosis through light–based technologies and machine learning

Doctoral Networks (MSCA-DN)

HORIZON - MSCA - 2022 - DN

Grant Agreement Nº 101119924

WP3: *Advanced microscopy for the analysis of cells and tissues involved in the development of diseases*

Deliverable D3.2

ONE analysis procedures

Rizzoli, UMG

Date: 21 09 2026

Type: R — Document, report.

Dissemination Level: PU-Public

Funded by the European Union

DELIVERABLE IDENTIFICATION SHEET

Document version	Date	Editor	Change(s)
1	21-09-2026	Rizzoli, Silvio	First version

Grant Agreement Nº	101119924
Call Identifier	HORIZON - MSCA - 2022 – DN
Acronym	BE-LIGHT
Full title	Improving biomedical diagnosis through light-based technologies and machine learning
Project URL	http://www.belightproject.eu/

Deliverable Nº and Name	D3.2 Functional analysis procedures based on ONE imaging of cerebrospinal fluid samples
Work Package	WP3 Advanced microscopy for the analysis of cells and tissues involved in the development of diseases
Lead Beneficiary	UMG
Type	R – Document, report.
Dissemination Level	PU-Public
Due date	Month 34

Authors (Partner)	Silvio Rizzoli, UMG			
Responsible Author	Silvio Rizzoli		**Email**	srizzol@gwdg.de
	Partner	UPC	**Phone**	+49 551 39 65911

Abstract (for dissemination)	Neurodegenerative diseases are often diagnosed late, only after specific symptoms are triggered by the removal of large groups of neurons. In the absence of early diagnosis, the patient faces inefficient symptomatic therapies, and does not have access to preventive therapies that could lengthen the pre-clinical, comfortable stage of life. This implies that the search for biomarker-based diagnostics is very important. Here we discuss the possibility of using two different super-resolution imaging approaches, ONE microscopy and STED microscopy, to image aggregates generated by alpha-synuclein, as a biomarker for Parkinson's Disease. We conclude that this is a promising approach, albeit substantial work is still necessary.
Keywords	STED, ONE microscopy, alpha-synuclein, Parkinson's Disease

Table of Contents

DELIVERABLE IDENTIFICATION SHEET **2**
EXECUTIVE SUMMARY **4**
INTRODUCTION **4**
1 SECTION 1 ..... **6**
1.1 Section 1.1 6
2 SECTION 2 ..... **11**
2.1 Section 2.1 11
3 SECTION 3 ..... **11**
3.1 Section 3.1 11
4 SUMMARY **13**
REFERENCES **13**
ANNEX **15**

EXECUTIVE SUMMARY

Super-resolution imaging of alpha-synuclein is a promising biomarker for Parkinson's Disease.

INTRODUCTION

The fight against neurodegenerative diseases is one of the most important global challenges of the current century, due to their increasing incidence and to their rising treatment costs. Most such diseases are diagnosed late, only after specific symptoms are triggered by the removal of large groups of neurons. In the absence of early diagnosis, based on sensitive biomarkers, the patient faces inefficient symptomatic therapies, and does not have access to preventive therapies that could lengthen the pre-clinical, comfortable stage of life. This implies that the search for biomarker-based diagnostics is very important.

Such diagnostics are especially relevant for Parkinson's disease (PD), a progressive neurodegenerative disease that shows both motor and non-motor impairment, including dementia, autonomic dysfunction and sleep disturbance. In principle, PD could be predicted by observing a number of clinical manifestations, including the loss of the sense of smell (Doty, 2012) or idiopathic REM sleep behaviour disorder (Postuma et al., 2015). While these are valuable markers, they lack specificity for PD (Postuma and Berg, 2016). Neuroimaging tools focusing on dopaminergic neurons in the substantia nigra have also been employed (Suwijn et al., 2015), albeit their scope is somewhat limited. Dopaminergic neuron dysfunction is not an early PD feature, being often preceded by non-motor features, caused by pathologic aggregation processes independent of dopamine neurons (Chahine et al., 2023).

In the last two decades, biomarker work in the PD field focused on the morphological abnormalities characteristic for this disease, including cytoplasmic inclusions (Lewy Bodies) and abnormal neuritic depositions (Lewy neurites). The principal component of these accumulations is the neuronal protein alpha-synuclein (αSyn; Schmitz et al., 2023). Lewy bodies or αSyn fibrils were initially thought to be the culprits in PD, simply due to their presence in the brains of affected individuals. However, more recent studies demonstrated that Lewy bodies are present in the surviving neurons, and can also be present in non-affected individuals. These observations suggest that smaller, oligomeric forms of αSyn might actually constitute the toxic agents (Gutierrez and Limon, 2022). This implies that, in principle, detecting the disease-relevant αSyn aggregate species is currently the best hope for PD diagnostic purposes and for monitoring disease progression. The different types of oligomers show different toxicity profiles (Yoo et al., 2022), implying that optimal diagnostics would detect the precise forms of oligomers from each patient, and not just a class of small, oligomer-like objects. Importantly, αSyn aggregates are also present in other diseases, as Dementia with Lewy bodies (DLB) and multiple systems atrophy (MSA). Their morphology is probably different, at both the tissue and the molecular levels (Van der Perren et al., 2020). An optimal diagnostic should differentiate between these diseases, by revealing their respective αSyn signatures.

A substantial number of studies focused on αSyn as a biomarker, with different levels of success. Genetic changes (mutations) in SNCA and its interacting partners made poor biomarkers, since familiar PD accounts for only a minority of all cases. Simply

measuring the αSyn levels has also proven to lack diagnostic relevance (Bruggink et al., 2011). Measuring post-translational modifications of αSyn (e.g. phosphorylation) has similarly been difficult to use as a biomarker (Magalhães and Lashuel, 2022). The combination of αSyn phosphorylation analyses with other parameters, including nerve fibre morphology, amyloid deposition and general skin histology, has been substantially more successful (Gibbons et al., 2023), leading to a commercial PD biomarker test (Syn-One TestTM, CND Life Sciences). However, it is unclear whether phosphorylated αSyn is a toxic species, since it seems to inhibit seeded fibril formation and toxicity (Ghanem et al., 2022), while also being a physiological form of αSyn, involved in synaptic transmission (Parra-Rivas et al., 2022).

Imaging oligomers directly, using oligomer-specific antibodies or electrochemical sensors, has been attempted (reviewed by Wang et al., 2023). It has been exceedingly difficult to identify the different types of oligomers, since the specificity of conformation-specific αSyn antibodies is highly contested (Kumar et al., 2020). Overall, such imaging experiments only result in the detection of small αSyn objects, but this is insufficient for diagnostic purposes (Magalhães and Lashuel, 2022). Importantly, αSyn-containing aggregates are present in the cerebrospinal fluid (CSF) and serum of both PD patients and controls (Lobanova et al., 2022). Thus, simply identifying aggregates (even oligomer-sized ones) is not useful for diagnostics: being able to reveal the toxic ones, the ones present specifically in PD patients, especially in early stages, would be much more valuable.

This issue has appeared impossible during the last decades, to the extent that the PD field has invested strongly in the direction of avoiding oligomer imaging altogether. One of the most important PD diagnostics tools, the seed amplification assay (SAA), does not target them at all, and relies simply on the presence of misfolded proteins (presumably αSyn) in the patient samples. In SAA experiments, the sample patients are mixed with purified, recombinant αSyn, which is induced to aggregate, forming fibrils that are then detected using amyloid-labelling dyes, as thioflavin-T (Bellomo et al., 2022). These assays, which include a commercial test (SYNTap®, Amprion), distinguish PD patients from controls with sufficient specificity and sensitivity, and could also separate disease types in the future, as PD and MSA, or PD and DLB (Okuzumi et al., 2023). They currently face several technical limitations, such as variation between laboratories and having their best performance in CSF, a material that is not suitable for screening (e.g. Borsche and Berg, 2023).

While these limitations may be solved in the future, the decision to ignore the exact nature of the toxic agents (the nature of the oligomers) limits the SAAs fundamentally, in several critical ways. First, SAAs so far provide a qualitative reading of the patient material (a yes/no answer to the presence of misfolded αSyn), lacking the ability to monitor molecule types and amounts. It is likely that the overall amounts of oligomers, and especially the amounts of individual oligomer subtypes, will provide a more precise analysis of disease stage, phenotype and/or progression. Second, only αSyn forms that aggregate into fibrils are detected in the current assays; it is unclear whether SAAs can detect oligomeric αSyn forms at all, and even less likely that SAAs can distinguish among individual oligomeric forms. Since oligomers may be the most toxic molecules, at least in the early disease stages, and recognition of individual αSyn forms may be relevant prognostically and in the development of therapeutics, these are serious limitations.

An assay in which all αSyn species would be detected and counted directly, without any amplification, would address all of these problems. Such a diagnostic would present the exact, personalized αSyn profile (αSyn signature) of each patient. It would therefore offer:

- Higher specificity, since the exact molecular phenotype of each patient would be discovered, and not just the categorical presence or absence of the αSyn forms detectable by SAA.

- Improved ability to follow disease progression, identifying changes in an individual patient's molecular phenotype over time, simply by monitoring the change in the numbers and morphologies of the αSyn forms.

- Higher sensitivity, as it would detect the αSyn objects at the single-molecule level, without the need to concentrate αSyn molecules by some means (e.g. immunoprecipitation).

- The ability to identify toxic αSyn forms earlier than other tests; large amounts of such forms, which can serve as seeds for SAA, are not necessary; identifying single molecules would be sufficient.

- A quantitative, and not just qualitative, readout, by counting different molecular forms precisely.

We present below this type of assay, based on the analysis of αSyn objects using expansion microscopy. This assay enabled us to correlate specific oligomers with patient medication, taken as a proxy for disease severity, and also revealed novel links between the patient condition and specific αSyn oligomers.

1 SECTION 1

Description of the imaging assay and its details: initial applications to CSF

1.1 Section 1.1

In principle, the PD field should be able to rely on fluorescence microscopy to analyse the αSyn oligomers. Unfortunately, optical imaging remains difficult to perform below 10-20 nm, which is the size of most αSyn oligomers. Several recent works have presented localization precisions down to 1-2 nm, or even below (Weber et al., 2022; Reinhardt et al., 2023; Sahl et al., 2023), but the application of such imaging resolution to biological samples has been severely limited by two fundamental problems. First, the achievable structural resolution is determined by the labelling density, which, in turn, is limited by the size of the fluorescent probes. As most αSyn detection experiments rely on antibodies, which are 10-15 nm in size, this implies that the resolution of the respective experiments is severely limited. Second, fluorophores can interact via energy transfer at distances below 10 nm, which lowers their localization probability (Helmerich et al., 2022).

The solution to these two problems would be to separate the fluorophores spatially by the physical expansion of the specimen, in what is termed expansion microscopy (ExM, Chen et al., 2015). To then reach the molecular scale, one would then combine ExM with optics-based super-resolution. This has been attempted numerous times, relying on

optics techniques such as STED, STORM or SIM, but the resulting performance typically reached only ~10 nm (e.g. Cahoon et al., 2017; Gao et al., 2018; Gambarotto et al., 2019). More recently, ExM has been combined with super-resolution approaches based on determining the higher-order statistical analysis of temporal fluctuations measured in a movie (e.g. Shaib et al., 2025). The resolution of these approaches is inversely correlated to the distance between the fluorophores, implying that they should benefit from ExM methodologies, in which fluorophores are separated from each other. The combination of 10-fold sample expansion (X10, Truckenbrodt et al., 2019) and super-resolution radial fluctuations (SRRF, Gustafsson et al., 2016) resulted in a technology with a resolution below 1 nm, which was termed one-step nanoscale expansion (ONE) microscopy (Shaib et al., 2025; Callaway, 2023).

ONE microscopy is easily applied to αSyn in human fluid samples, where it can differentiate between PD patients and controls. To our knowledge, this is the only current technology that is able to reveal the morphologies of the different oligomeric species in human fluids. In brief, the samples are attached to a gel-compatible anchor, typically through amine-derivatization chemistry, and are then embedded into a swellable X10 gel. Sample homogenization is performed by proteinase K treatments or by heating in alkaline buffers, leading to peptide chain breaks and enabling the isotropic 10-fold expansion of the sample, which is achieved by incubating the gels with distilled water (Truckenbrodt et al., 2019). The samples are then imaged using confocal microscopy, acquiring series of images (movies) of hundreds to thousands of images (ideally 1500-5000), in which fluctuations of the fluorescence intensity are observed (Shaib et al., 2025). The resulting movies are the analysed following the SRRF procedure (Gustafsson et al., 2016). In theory, the precision of the SRRF technique should reach values close to 10 nm (Gustafsson et al., 2016). In practice, most previous implementations of SRRF have reached only ~50-70 nm, implying that its combination with 10-fold expansion should only reach resolutions of ~5-7 nm. Expansion by 10-fold, however, removes two major limitations of SRRF: it separates overlapping fluorophores, enabling them to fluctuate independently, and improves the signal-to-noise ratio. This enables SRRF to reach its theoretical performance, which, when combined with the expansion factor, results in molecular-scale imaging (~1 nm).

To analyse αSyn in ONE microscopy, CSF from PD patients and similarly aged controls was collected and was immunostained (Fig. 1), using a nanobody (De Genst et al., 2010). Nanobodies represent the single-domain variable fragments of IgG2/3 antibody subtypes that are absent in most mammals, but are found in camels and llamas. Their coding sequence can be revealed by dedicated in vitro procedures (Vincke and Muyldermans, 2012). Antibodies cannot be used in this type of analysis, since their large size reduces the precision of the microscopy.

Examples of ONE images of αSyn objects from human CSF are shown in Fig. 2. Different types of objects were detected, and PD patients had higher levels of oligomer-like structures (Fig. 2A-C). An initial classification of these structures was performed, separating them into “very large” assemblies (>200 nm in length, >50 nm in width), “large” assemblies (50 to 200 nm in length), and oligomers of different morphologies. The first two types of assemblies were found at similar frequency in PD patients and controls (Fig. 2D). However, this was not the case for the smaller, oligomer-like assemblies. Some resembled strikingly polymorphic αSyn assemblies that have been described by Cryo-EM in recombinant αSyn samples (Guerrero-Ferreira et al., 2019; Li

et al., 2018), while others had an annular organization as observed in the past by negative stain electron microscopy or Cryo-EM (e.g. Zhang et al., 2013). All oligomer-like species were significantly more abundant in PD CSF than in control samples (Fig. 2E), and their cumulative analysis was shown to result in discrimination of PD patients and controls (Fig. 2F,G). Importantly, due to local ethical regulations, the controls were not healthy persons, but patients with non-PD neurological disorders, which are thought to be more difficult to differentiate from PD patients than healthy persons.

Importantly, different αSyn species are associated with clinical features of PD (Fig. 2H). Due to space limitations, we can provide only a few such examples here. We compared PD patients receiving levodopa/decarboxylase inhibitor therapy (LD/DCI) to untreated patients. LD/DCI therapy indicates great disease severity, and has been used as an outcome measure in neuroprotective trials (e.g. Parkinson Study Group, 1989). The numbers of large assemblies (up to ~200 nm in length) were more frequent in PD patients not receiving LD/DCI (lower severity) when compared to patients with greater severity, receiving LD/DCI treatment, suggesting that the number of large assemblies may be inversely correlated with severity. In contrast, two oligomers, types 3 and 5, were more common in more advanced PD patients treated with LD/DCI, suggesting that these oligomers may have greater toxicity. This hypothesis is further supported by the observation that type 3 oligomers are also associated with an inflammatory phenotype, which has been associated with PD progression. Finally, the annular oligomers correlate well with the immunoglobulin A (IgA) levels in the CSF, which could be regarded as an additional marker of inflammation. In PD, immune mechanisms are complex, and are thought to interact with genes and environment to mediate the onset and progression of PD (Tansey et al., 2022). In a recent study, the more severe akinetic rigid PD phenotype was associated with a microbiome IgA signature, providing indirect evidence that this immune marker may be correlated with disease phenotype (Brown et al., 2023).

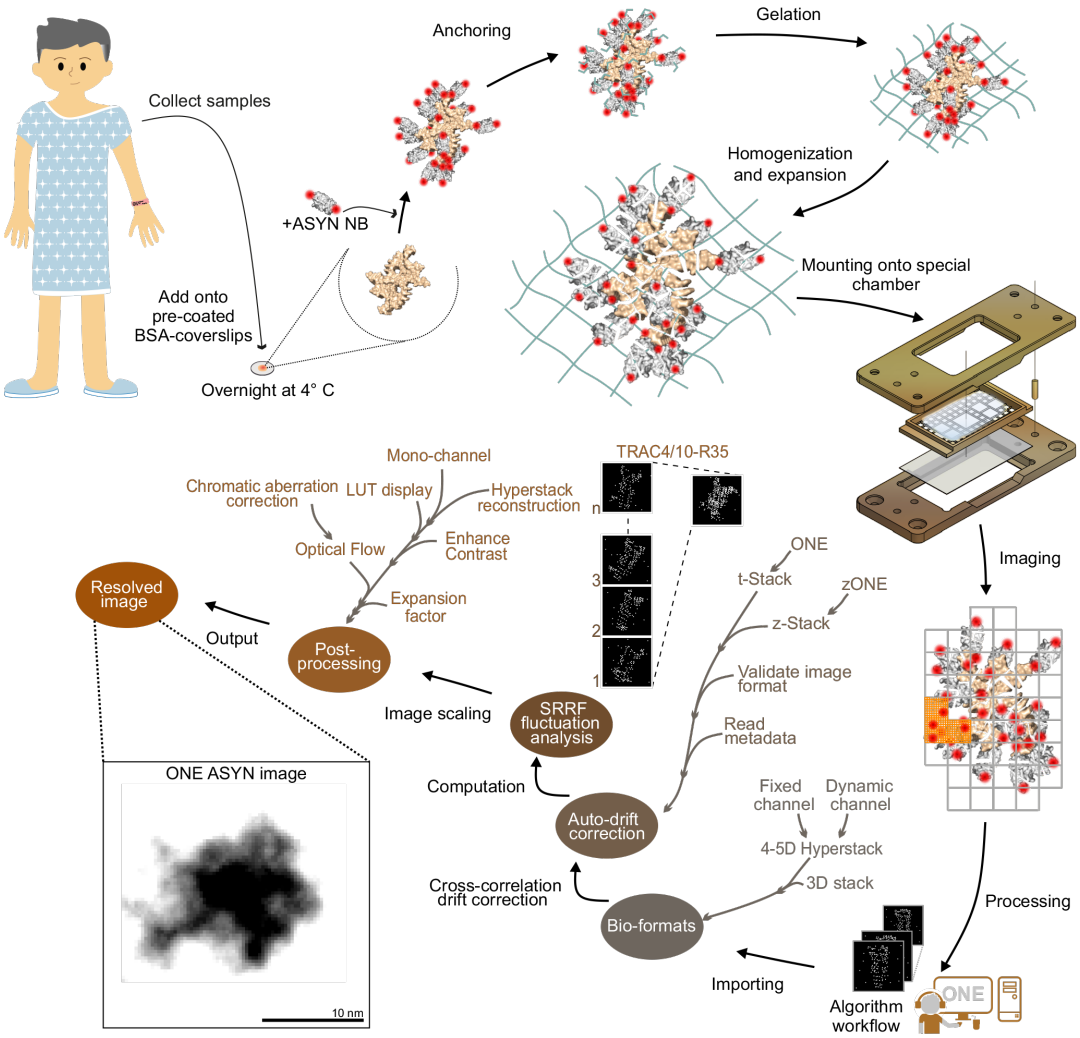

Fig. 1. A general overview of the ONE microscopy approach. *Cerebro-spinal fluid or serum probes were obtained from PD patients and controls, and 20 µl amounts were placed on BSA-coated coverslips. They were then linked to gel anchors, relying on Acryloyl-X, followed by X10 gel formation and homogenization, either by proteinase K additions or by autoclaving in alkaline buffers. Full expansion was achieved by repeated washes, and was followed by mounting gel portions in a specially designed chamber. The samples were then imaged, capturing up to 5000 images, to detect signal fluctuations, which were then computed using a SRRF algorithm, before assembling the final super-resolved images. The different algorithm steps are described in the scheme. An individual αSyn oligomer is shown, as an example.*

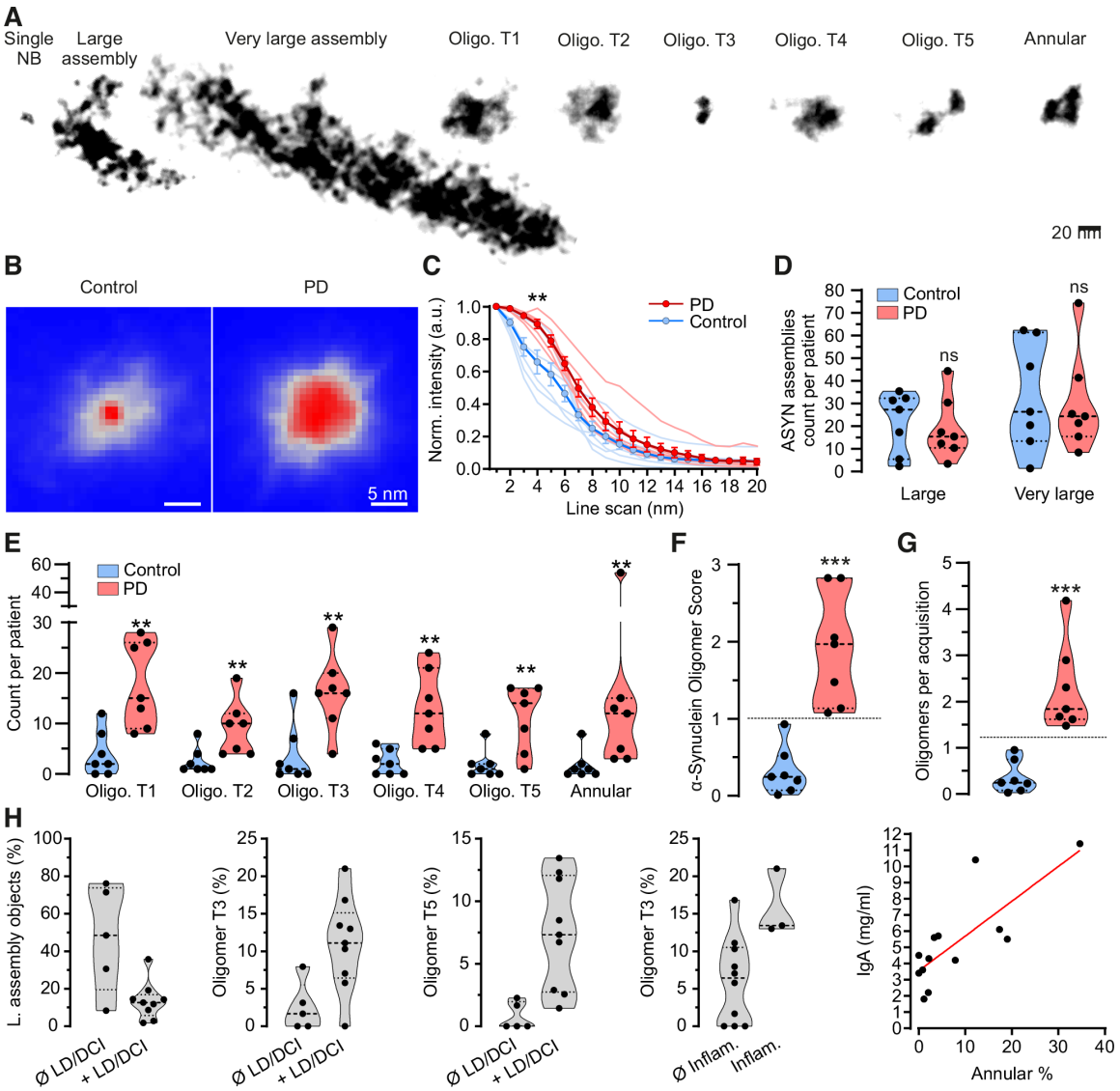

Figure 2. αSyn analysis in CSF. ***A)*** *A gallery of typical αSyn species observed in CSF samples.* ***B)*** *Average αSyn assemblies from a PD patient and a control.* ***C)*** *An analysis of the spot profiles detects significant differences (7 control and 7 PD patients; Friedman test followed by Dunn-Sidak, p = 0.0237; errors show SEM).* ***D)*** *An analysis of the numbers of the larger assemblies in CSF samples. No significant differences, Mann-Whitney tests, p>0.1.* ***E)*** *An analysis of the numbers of oligomers in CSF samples. All comparisons indicate significant differences, Mann-Whitney tests followed by a Benjamini-Hochberg multiple testing correction with FDR of 2.5%; p<0.013 for all datasets.* ***F,G)*** *Analyses of the numbers of oligomers, as a proportion of all αSyn assemblies (F), or as numbers per acquisition (G; Mann-Whitney test, p<0.0001 for both panels). Both procedures discriminate fully between PD patients and controls.* ***H)*** *Large assemblies correlate inversely with LD/DCI treatments; oligomer types 3 and 5 correlate positively with these treatments (Mann-Whitney tests followed by a Benjamini-Hochberg multiple testing correction with FDR of 5%; p<0.017 for all three datasets). Type 3 also correlates significantly with brain inflammation (p=0.021). Annular oligomers correlate well with IgA levels in CSF (p = 0.0015, Pearson correlation test).*

2 SECTION 2

ONE microscopy applications to serum samples

2.1 Section 2.1

The use of CSF as the fluid of choice for these analyses is not ideal, since CSF is obtained through procedures that are associated with a level of risk for the patient, rendering it unsuitable for routine screening. To address this problem, more easily obtained fluids, as blood (serum), tears and saliva have been considered as a source of αSyn for medical testing (Magalhães, & Lashuel, 2022). We turned to serum samples, and performed the same type of analysis. Differences between PD patients and controls were again readily observed, implying that mapping the αSyn signature by ONE microscopy is a promising avenue.

3 SECTION 3

Recent work on non-expanded samples

3.1 Section 3.1

The main difficulty in analyzing ONE microscopy samples is that their number is limited by the fact that the expansion microscopy procedure is relatively slow, and can address only a limited number of samples in parallel.

Therefore, we analyzed a considerable number of samples, using non-expanded material, imaged by STED microscopy. In brief, we turned to a classical procedure, which we performed earlier for Alzheimer's Disease, using CSF samples (Zhang et al., 2015), which has a high enough precision to allow the discrimination of different objects with sizes down to approximately 40-50 nm. We obtained serum samples from PD patients and controls, and we proceeded as follows:

- We labeled the samples using the same nanobodies as described above, and we then imaged the coverslips by STED microscopy.
- We segmented the images, using a thresholding procedure, and identified the different objects, as local maxima in the images.
- We determined the size and intensity of each object, using Gaussian fitting procedures.
- We compared the distribution of the 1) size and 2) intensity of the objects in different patients.
- We also examined the following parameters: 3) the distance from each αSyn spot to its nearest neighbor; 4) the size and 5) the intensity of the nearest neighbor; 6) the average distance from each αSyn spot to its neighboring population (spots within 400 nm of itself); 7) the average size, 8) the average intensity of the neighboring population, 9) the number of neighboring particles within 400 nm; 10-13) similar parameters to 6-9, for the neighboring population found within distances of 400 to 1000

nm; 14-17) similar parameters to 6-9, for the neighboring population found within distances of 1000 to 2000 nm.

- All of these 8 parameters were compared to each other, in the form of two-dimensional scatter plots. The two-dimensional scatter plots were converted to two-dimensional histograms, comparing the following sets of parameters to each other:
  - Spot size vs. intensity
  - Nearest-neighbor distance vs. spot intensity
  - Nearest-neighbor intensity vs. spot intensity
  - Nearest-neighbor distance vs. spot size
  - Nearest-neighbor size vs. spot size
  - Nearest-neighbor population average size vs. nearest-neighbor population average intensity
  - Nearest-neighbor population average distance vs. nearest-neighbor population average intensity
  - Nearest-neighbor population average intensity vs. spot intensity
  - Nearest-neighbor population average distance vs. nearest-neighbor population average size
  - Nearest-neighbor population average size vs. spot size
  - Spot intensity vs. nearest-neighbor size
  - Nearest-neighbor population average intensity vs. nearest-neighbor size
  - Nearest-neighbor population average size vs. nearest-neighbor size
  - Nearest-neighbor population average intensity vs. nearest-neighbor distance
  - Nearest-neighbor population average size vs. nearest-neighbor distance
  - Nearest-neighbor population average distance vs. nearest-neighbor distance
  - Nearest-neighbor population average distance vs. spot intensity
  - Nearest-neighbor population average distance vs. spot size
  - Spot size vs. nearest-neighbor intensity
  - Nearest-neighbor population average intensity vs. nearest-neighbor intensity
  - Spot size and intensity vs. the number of neighboring particles within 400 nm
  - Spot size and intensity vs. the average distance, size, intensity and number of particles for the neighboring particles within 400-1000 nm
  - Spot size and intensity vs. the average distance, size, intensity and number of particles for the neighboring particles within 1000-2000 nm
- The two-dimensional histograms were combined in one single histogram, by simply linking all matrices into one.
- Further combinations and comparisons of parameters will continue to be tested, to improve the discrimination procedure.

- These matrices were compared between PD patients and their controls, relying on a training cohort of PD patients and similar-age controls.
- We determined the comparison classes (specific size vs. intensity, nearest neighbor distance vs. intensity, etc.) that tended to be different between PD patients and controls, and computed their abundance into a discrimination parameter, for which we summed the abundances of all objects that were more abundant in one category (e.g. PD) and we subtracted the abundances of all objects that were less abundant in the respective category. This results in a discrimination parameter whose cutoff is approximately -10 arbitrary units, and which provided a sensitivity and specificity of ~94% in the training cohort.

We are now in the process of improving this analysis, and applying it to further, test cohorts.

4 SUMMARY

Neurodegenerative diseases are often diagnosed late, only after specific symptoms are triggered by the removal of large groups of neurons. In the absence of early diagnosis, the patient faces inefficient symptomatic therapies, and does not have access to preventive therapies that could lengthen the pre-clinical, comfortable stage of life. This implies that the search for biomarker-based diagnostics is very important. Here we discuss the possibility of using two different super-resolution imaging approaches, ONE microscopy and STED microscopy, to image aggregates generated by alpha-synuclein, as a biomarker for Parkinson's Disease. We conclude that this is a promising approach, albeit substantial work is still necessary.

REFERENCES

Bellomo G, De Luca CMG, Paoletti FP, Gaetani L, Moda F, Parnetti L (2022) *Neurology* **99**: 195-205.

Borsche M, Berg D (2023) *Mov Disord* **38**: 1397-1398.

Brown EL, Essigmann HT, Hoffman KL, Alexander AS, et al (2023) *J Parkinsons Dis* 13: 501-513.

Bruggink KA, Kuiperij HB, Ekholm-Pettersson F, Verbeek MM (2011) *Neurology* **77**: 510-511.

Chen F, Tillberg PW, Boyden ES (2015) *Science* **347**: 543-548.

Cahoon CK, Yu Z, Wang Y, Guo F, Unruh JR, et al. (2017) *Proc Natl Acad Sci U S A* **114**: E6857-E6866.

Callaway E (2023) *Nature* **616**: 417-418.

Chahine LM, Merchant K, Siderowf A, Sherer T, Tanner C, Marek K, et al. (2023) *J Parkinsons Dis* **13**:297-309.

De Genst EJ, Guilliams T, Wellens J, O'Day E, et al. (2010) *J Mol Biol* **402**: 326-343.

Gambarotto D, Zwettler FU, Le Guennec M, Schmidt-Cernohorska M, et al. (2019) *Nat Methods* **16**: 71-74.

Gao M, Maraspini R, Beutel O, Zehtabian A, Eickholt B, Honigmann A, Ewers H (2018) *ACS Nano* **12**: 4178-4185.

Ghanem SS, Majbour NK, Vaikath NN, Ardah MT, et al. (2022) *Proc Natl Acad Sci U S A* **119**: e2109617119.

Gibbons C, Wang N, Rajan S, Kern D, Palma JA, Kaufmann H, Freeman R (2023) *Neurology* **100**: e1529-e1539.

Guerrero-Ferreira R, Taylor NM, Arteni AA, Kumari P, Mona D, et al. (2019) *Elife* **8**: 48907.

Gustafsson N, Culley S, Ashdown G, Owen DM, Pereira PM, et al. (2016) *Nat Commun* **7**: 12471.

Gutierrez BA, Limon A (2022) *Biomedicines* **10**:1743.

Helmerich DA, Beliu G, Taban D, Meub M, Streit M, et al. (2022) *Nat Methods* **19**: 986-994.

Kumar ST, Jagannath S, Francois C, Vanderstichele H, Stoops E, Lashuel HA (2020) *Neurobiol Dis* **146**:105086.

Li B, Ge P, Murray KA, Sheth P, Zhang M, Nair G, Sawaya MR, et al. (2018) *Nat Commun* **9**: 3609.

Lobanova E, Whiten D, Ruggeri FS, Taylor CG, Kouli A, Xia Z, Emin D, et al. (2022) *Brain* **145**: 632-643.

Magalhães P, Lashuel HA (2022) *NPJ Parkinsons Dis* **8**: 93.

Okuzumi A, Hatano T, Matsumoto G, Nojiri S, Ueno SI, Imamichi-Tatano Y, et al. (2023) *Nat Med* **29**: 1448-1455.

Parra-Rivas LA, Madhivanan K, Wang L, et al. (2022) *BioRxiv* doi: https://doi.org/10.1101/2022.12.22.521485

Parkinson Study Group (1989) *N Engl J Med* **321**: 1364-1371.

Postuma RB, Berg D (2016) *Nat Rev Neurol* **12**: 622-634.

Postuma RB, Gagnon JF, Bertrand JA, Génier Marchand D, Montplaisir JY (2015) *Neurology* **84**: 1104-1113.

Reinhardt SCM, Masullo LA, Baudrexel I, Steen PR, Kowalewski R, et al. (2023) *Nature* **617**: 711-716.

Sahl SJ, Matthias J, Inamdar K, Khan TA, et al. (2023) *BioRxiv* doi: https://doi.org/10.1101/2023.07.07.548133

Schmitz M, Candelise N, Canaslan S, et al. (2023) *Transl Neurodegener* **12**:12.

Shaib AH, Chouaib AA, Imani V, Chowdhury R, et al. (2025) *Nat Biotechnol* **43**:1539-1547.

Suwijn SR, van Boheemen CJ, de Haan RJ, Tissingh G, Booij J, de Bie RM (2015) *EJNMMI Res* **5**:12.

Tansey MG, Wallings RL, Houser MC, Herrick MK, Keating CE, Joers V (2022) *Nat Rev Immunol* **22**: 657-673.

Truckenbrodt S, Sommer C, Rizzoli SO, Danzl JG (2019) *Nat Protoc* **14**: 832-863.

Van der Perren A, Gelders G, Fenyi A, Bousset L, Brito F, et al. (2020) *Acta Neuropathol* **139**: 977-1000.

Vincke C, Muyldermans S (2012) *Methods Mol Biol* **911**: 15-26.

Wang R, Pang SC, Li JY, Li CL, Liu JM, Wang YM, et al. (2023) *Anal Bioanal Chem* **415**: 1589-1605.

Weber M, von der Emde H, Leutenegger M, et al. (2022) *Nat Biotechnol* doi:10.1038/s41587-022-01519-4.

Yoo JM, Lin Y, Heo Y, Lee YH (2022) *Front Mol Biosci* **9**: 959425.

Zhang H, Griggs A, Rochet JC, Stanciu LA (2013) *Biophys J* **104**: 2706-2713

Zhang WI, Antonios G, Rabano A, Bayer TA, Schneider A, Rizzoli SO (2015). *J Alzheimers Dis* **46:**1007-20

ANNEX